QUARTERLY OF APPLIED MATHEMATICS
VOLUME LI, NUMBER 1
MARCH 1993, PAGES 129–146

NONLINEAR VORTEX TRAIL DYNAMICS PART II: ANALYTIC SOLUTIONS

BY

CHJAN C. LIM (*Rensselaer Polytechnic Institute, Troy, New York*)

AND

LAWRENCE SIROVICH (*Brown University, Providence, Rhode Island*)

Abstract. Spatially periodic large amplitude solutions of the von Karman model are obtained in the neighborhood of singularities. These singularities correspond to vortex clusters in the physical plane. The quasi-periodic and unbounded solutions found analytically confirm earlier numerical work and show qualitative agreement with experimental observations of large-scale phenomena of vortex trails. Separatrices or heteroclinic orbits were explicitly found for an integrable approximate equation, which indicate that the von Karman model itself supports chaotic solutions.

0. Introduction. The large-scale motions of the vortex trail shed by a cylindrical bluff object include vortex-merging in the near wake such as the formation of opposite signed vortex couples (so-called Batchelor couples) and clusters of three or more vortices. These were observed by Basdevant, Couder, and Sadourny [2] in elegant soap film experiments (cf. also Matsiu and Okude [10]). The vortices in the near wake have finite cores, which are arranged in two staggered rows. Moreover, viscosity plays a role in the wake. In this paper and Lim and Sirovich [9] (henceforth paper I), we ask the question:

I. Are viscosity, three-dimensionality, and finite cores second-order factors in the *large-scale motions* of the vortex trail?

Clearly, these factors dominate the finer scales in the flow. This question is equivalent to:

I′. Does the von Karman model have enough structure to account for the large scale nonlinear phenomena described in the above experiment?

The von Karman model was formulated in 1911 [15] and was partially successful in explaining some of the linear phenomena of the vortex trail. More recently, linear solutions (both periodic and aperiodic) of the model were compared with the evidence for wave propagation in the vortex trail [8, 12–14].

Received April 19, 1991.
1991 *Mathematics Subject Classification.* Primary 70F10, 76C05; Secondary 34C28, 34D99, 70H05.
This work was supported by NASA under Grant No. 5-28547 and by DARPA URI, No. 5-28575, and by NSF under Grant No. DMS-9006091.

In paper I, we discussed some of the large-amplitude spatially periodic solutions of the fully nonlinear von Karman model *numerically*, using the four-group case of Kochin's Hamiltonian (2). The four-group case was analyzed mainly because approximately four-group motions, both quasi-steady and unbounded, were actually observed in experiments. Moreover, it is the shortest wavelength disturbance for a 1-D lattice such as the von Karman model (which makes the four-group the easiest case). Clearly, the other cases, of longer wavelength, should also be studied. Numerical integration demonstrated that the spatially periodic solutions of the von Karman model consist of a rich variety of large-amplitude nonlinear behaviour. In paper I, we remarked on the qualitative agreement between our results and the experimental observations noted above.

However, the analysis of question I′ in paper I cannot be regarded as complete without a mathematical analysis of the four-group Kochin's equations (1), if such an analysis is possible. The analysis in this paper will not only confirm the rich variety of *regular* solutions found numerically but also demonstrate the possibility of *chaotic behaviour* in the von Karman model.

In Sec. 1, we recall the Hamiltonian formulation of Kochin [4] and describe the singularities of Hamilton's equations. The singularities, which represent vortex cluster, play central roles in the numerical integration in paper I and in the following analysis. In Secs. 2 and 3, we discuss the unbounded solutions of (1). Section 4 contains the main results: (a) existence of quasi-periodic solutions of (1) in the neighborhood of a singularity, which correspond to dynamic clusters of three vortices in configuration space, and (b) existence of a separatrix (heteroclinic orbit). In Secs. 5 and 6, quasi-periodic solutions in the neighborhood of other singularities are found. We use the methods of classical mechanics and dynamical system theory in the following analysis.

1. Singularities and vortex clusters. We recall Kochin's equations [4, 9],

$$\begin{aligned} \frac{d\bar{\alpha}}{d\tau} &= -4i \sin\beta \left[\frac{1}{\cos\alpha + \cos\beta} - \frac{1}{\cos\beta - i} \right], \\ \frac{d\bar{\beta}}{d\tau} &= -4i \sin\alpha \left[\frac{1}{\cos\alpha + \cos\beta} - \frac{1}{\cos\alpha + i} \right]. \end{aligned} \tag{1}$$

The complex quantities α, β represent the normalized relative positions of the positions of the vortices in the unit cell (four-group). A standard reduction has been used to obtain this two-degrees-of-freedom Hamiltonian system for the Hamiltonian function,

$$H(\alpha, \beta) = -4 \ln \left| \frac{(\cos\alpha + i)(\cos\beta - i)}{\cos\alpha + \cos\beta} \right|. \tag{2}$$

The singularities of (2) correspond to the values of (α, β) for which the following factors vanish:

$$\begin{aligned} \cos\alpha + i = 0 &\to \alpha = \pm \left(\frac{\pi}{2} + i \sinh^{-1}(1) \right) \equiv \pm\alpha_0, \\ \cos\beta + i = 0 &\to \beta = \pm \left(\frac{\pi}{2} + i \sinh^{-1}(1) \right) \equiv \beta, \\ \cos\alpha + \cos\beta = 0 &\to \alpha_1 = \pm\beta_1 + (2n+1)\pi, \qquad n \text{ an integer.} \end{aligned}$$

These singularities correspond to collisions of vortices. Hence, the neighborhood of singularities corresponds to vortex clusters in the physical plane, which are illustrated case-by-case in Fig. 3 of paper I.

Although (1) is not completely integrable, our strategy in this paper is to write (1) in the form of separate *nearly integrable* equations in the neighborhood of the singularities. The integrable part is solved completely, then the bounded solutions such as quasi-periodic orbits on tori are continued to the full equation (1) in a sufficiently small neighborhood of the associated singularity (cf. also [6, 7, 1, 11]).

2. Unbounded solution and collision of vortex trails. We first consider unbounded solutions of Kochin's equations. If we assume that imaginary parts become unbounded then it is clear from the form of the Hamiltonian (2) that only one of α, β can have a divergent imaginary part. It follows from the symmetry (20) in paper I that no generality is lost in taking $\mathrm{Im}(\alpha)$ as becoming unbounded.

To be specific, suppose $\alpha_i > 0$ (and large). Then since $\cos\alpha = O(e^{\alpha_i})$, it follows that Kochin's equations take the form

$$\begin{aligned} \frac{d\overline{\alpha}}{d\tau} &= \frac{4i\sin\beta}{\cos\beta - i} + O(e^{-\alpha_i}), \\ \frac{d\overline{\beta}}{d\tau} &= O(e^{-\alpha_i}) \end{aligned} \tag{3}$$

for $|\alpha_i|$ large. This implies that growing solutions have the form

$$\begin{aligned} \alpha &= \omega\tau + \alpha^o + o(\tau^{-n}), \\ \beta &= \beta_\infty + o(\tau^{-n}) \end{aligned} \tag{4}$$

for all $n > 0$. Substituting into Kochin's equation (1), yields

$$\overline{\omega} = \frac{4i\sin\beta_\infty}{\cos\beta_\infty - i}, \tag{5}$$

which relates the complex growth rate ω to the limiting value for β, i.e., β_∞. These asymptotic states (4) of Kochin's equation are directly related to the unbounded numerical solutions described in paper I, Fig. 4. From the definition of α, β in terms of the separation between rows, the asymptotic states (4) correspond to two vortex trails moving apart. Each vortex trail consists of two rows of opposite circulation and in general is not perfectly staggered, which implies vertical velocities.

This asymptotic behavior can be conveniently discussed in terms of the *collision of vortex trails.* For this purpose observe that the Hamiltonian (2) has the asymptotic form

$$H_\infty = -4\ln|\cos\beta - i| + O(e^{-\alpha_i}). \tag{6}$$

(A similar expression holds if instead $|\beta_i| \gg 1$.) In the limit as $\tau \to \infty$, the unbounded solution, with α_i becoming unbounded, must satisfy

$$H_\infty = -4\ln|\cos\beta_\infty - i| = H(\alpha, \beta) \tag{7}$$

where $H(\alpha, \beta)$ is the exact Hamiltonian (2).

Since Kochin's equation is reversible, unbounded solutions can be retraced to $\tau = -\infty$. At such time when variables α, β are $O(1)$, full interaction occurs between the four rows. The possible outcomes of such scattering interaction can be characterized in terms of their asymptotic states as $\tau \to -\infty$. For the case where α_i grows at $\tau = \infty$, these are:

(a) α_i also grows like $O(\tau) = -\infty$ while $\beta \to \beta_{-\infty}$. Neither the growth rate of α_i nor $\beta_{-\infty}$ need be the same as when $\tau = \infty$. In this case, the pair of interacting vortex trails scatter without exchanging rows.

(b) β_i grows linearly while $\alpha \to \alpha_{-\infty}$. From the definition of the variables (α, β) in terms of the separations between vortex rows, this means the pair of interacting vortex trails exchange rows in such a scattering process.

(c) Only the real parts of the variables (α, β) grow. In this scattering process, the pair of vortex trails remain near to each other in the physical plane since α_i, β_i are bounded. Further the four rows slide continuously in the horizontal direction.

(d) All variables (α, β) are bounded. The four rows engage in a continuous shuffling motion.

In the first two cases, respectively, the conservation of Hamiltonian implies that

(a) $H_{-\infty} = -4 \ln |(\cos \beta_{-\infty} - i)| = H_{\infty} = -4 \ln |(\cos \beta_{\infty} - i)|$, which implies

$$|\cos \beta_{-\infty} - i| = |\cos \beta_{\infty} - i|; \tag{8}$$

(b) $H_{-\infty} = -4 \ln |(\cos \beta_{-\infty} - i)| = H_{\infty} = -4 \ln |(\cos \alpha_{\infty} + i)|$, which implies

$$|\cos \beta_{-\infty} - i| = |\cos \alpha_{\infty} + i|. \tag{9}$$

Aside from the simple geometrical condition (8) or (9), nothing can be said to relate the states at $\tau = \pm\infty$. From given initial data, which is $O(1)$, there does not appear to be a direct way to predict the asymptotic states. Numerical integration of Kochin's equations, which depict scattering phenomena, are described in paper I.

Now we observe that unbounded solutions occur for any value of the Hamiltonian. To see this we start with (5), from which we see that β_{∞} must be such that

$$\omega_i(\beta_{\infty}) = \frac{\cos \beta_{\infty_r} (4 \sin \beta_{\infty_r} - 4 \sinh \beta_{\infty_i})}{|(\cos \beta_{\infty} - i)|^2} \tag{10}$$

for unbounded solutions to exist. For any given value of H, (7) yields

$$\cos \beta_{\infty} = i + e^{i\theta} e^{-H/4} \tag{11}$$

where θ is real and arbitrary. It is clear that for any H, there are values of β_{∞} from (11) for which the numerator of (10) is not equal to zero because the terms $\sin \beta_{\infty_r}$ and $-\sinh \beta_{\infty_i}$ can be chosen to have the same sign. Thus for any value of the Hamiltonian, there are unbounded solutions for Kochin's equations.

3. Vortex merging: Couples. In paper I we found a singularity of (1) which, in the physical plane, corresponded to the merging of two rows of opposite circulation. (An illustration is given in Fig. 3a of paper I). We now consider the solution of Kochin's equations when (α, β) lie in the neighborhood of such a singularity. In particular,

we take α bounded away from $\pm\alpha_0 = \pm(\frac{\pi}{2} + i\pi k_0)$ and

$$\beta \approx \pm\beta_0 = \pm\left(\frac{\pi}{2} - i\pi k_0\right). \tag{12}$$

We therefore assume that, at some instant,

$$\left|\frac{\cos\beta - i}{\cos\alpha + i}\right| \ll 1. \tag{13}$$

If we rewrite Kochin's equations in the form

$$\begin{aligned}\dot{\bar{\alpha}} &= \frac{-4i\sin\beta(\cos\alpha + i)}{(\cos\alpha + \cos\beta)(\cos\beta - i)},\\ \dot{\bar{\beta}} &= \frac{-4i\sin\alpha(\cos\beta - i)}{(\cos\alpha + \cos\beta)(\cos\alpha + i)}\end{aligned} \tag{14}$$

expansion yields

$$\begin{aligned}\dot{\bar{\alpha}} &= \frac{-4i\sin\beta}{\cos\beta - i}\left[1 - \left(\frac{\cos\beta - i}{\cos\alpha + i}\right) + \cdots\right],\\ \dot{\bar{\beta}} &= \frac{-4i\sin\alpha(\cos\beta - i)}{(\cos\alpha + i)^2}\left[1 - \left(\frac{\cos\beta - i}{\cos\alpha + i}\right) + \cdots\right].\end{aligned} \tag{15}$$

For the case (12), it is easy to show that $\sin\beta$ is $O(1)$. Since (13) holds at some instant, we ignore all but the leading term in (15). Thus, it is clear that at this instant

$$\begin{aligned}\dot{\bar{\alpha}} &= \bar{\omega}(\beta) = \frac{-4i\sin\beta}{\cos\beta - i} = O\left(\frac{1}{\varepsilon}\right),\\ \dot{\bar{\beta}} &= \frac{-4i\sin\alpha}{\cos\alpha + i}\left(\frac{\cos\beta - i}{\cos\alpha + i}\right) = O(\varepsilon).\end{aligned} \tag{16}$$

Therefore, if $\operatorname{Im}\omega \neq 0$, β will tend to a constant $\beta^0 \approx \pm\beta_0$ exponentially while α grows linearly at the rate $\omega(\beta^0)$. The solution has the same form as the data (12) and condition (13), which justifies the expansion (15) holds for all time.

Without assuming that initial data is large as we did in Sec. 2, we have found unbounded solutions of Kochin's equations that tend to asymptotic states similar to (4) except the constant value of β is close to the singular values, $\pm\beta_o$. These unbounded solutions correspond to the rapid migration of vortex couples from the Karman trail. This is to be compared with the numerical integration of Kochin's equations with initial data such as (12) (cf. paper I, Fig. 6).

4. Quasi-periodic solution and heteroclinic orbits. In the neighborhood of the case 2 singularity where

$$(\alpha, \beta) \approx (\alpha_0, \beta_0) = \left(\frac{\pi}{2} + i\sinh^{-1}(1), \frac{\pi}{2} - i\sinh^{-1}(1)\right), \tag{17}$$

Kochin's equations (1) take the form

$$\begin{aligned}\dot{\bar{a}} &= \frac{-4i(\sqrt{2}\cos b + i\sin b)(-i\cos a - \sqrt{2}\sin a + i)}{(-i\cos a + i\cos b - \sqrt{2}\sin a - \sqrt{2}\sin b)(i\cos b - \sqrt{2}\sin b - i)},\\ \dot{\bar{b}} &= \frac{-4i(\sqrt{2}\cos a - i\sin b)(i\cos b - \sqrt{2}\sin b - i)}{(-i\cos a + i\cos b - \sqrt{2}\sin a - \sqrt{2}\sin b)(-i\cos a - \sqrt{2}\sin a + i)}\end{aligned} \tag{18}$$

if we write

$$a = \alpha - \alpha_0 , \qquad b = \beta - \beta_0 \tag{19}$$

and use $\sin\alpha_0 = \sin\beta_0 = \sqrt{2}$. We can proceed in a similar way for all the subcases $(\pm\alpha_0, \pm\beta_0)$. On expanding the trigonometric terms in the Hamiltonian function (2), we obtain the nearly integrable form

$$H(a, b) = H_0(a, b) + H_1(a, b) \tag{20}$$

where the perturbation term is quadratic in $|a|$, $|b|$; i.e., H_1 is the sum of three terms having the form

$$8 \ln |1 + O(|a|^2, |b|^2, |a||b|)|.$$

The leading terms in the expansion of (18),

$$\dot{\bar{a}} = \frac{4ia}{b(a+b)} , \qquad \dot{\bar{b}} = \frac{4ib}{a(a+b)} , \tag{21}$$

are Hamilton's equations,

$$\dot{\bar{a}} = i\frac{\partial H_0}{\partial b} , \qquad \dot{\bar{b}} = i\frac{\partial H}{\partial a} , \tag{22}$$

for the unperturbed Hamiltonian function

$$H_0 = 8 \ln \left| \frac{ab}{a+b} \right| . \tag{23}$$

There are two steps in the procedure to establish the result:

> (A) There exists a "large" (in the sense of Lebesgue measure in phase-space) set of quasi-periodic solutions of (1) in a sufficiently small neighborhood of the singularity (17). Moreover, these solutions of (1) are very close to the solutions of (21).

Step I. We will show that (21) is *completely integrable*, that is, it has an independent invariant in involution with H_0, and then solve (21) explicitly in terms of elliptic integrals. These solutions, summarized in Fig. 1, have the form of a family of bounded solutions enveloped by separatrices (heteroclinic orbits) that connect two hyperbolic fixed points, given in polar coordinates (24) by

$$\rho \equiv \frac{R_b}{R_a} = 1 , \qquad \Theta = \theta_b - \theta_a = \pm\frac{2\pi}{3} .$$

Since (21) (and the full equations (1), (18)) have two degrees of freedom, Fig. 1 is the Poincaré section of the flow on the 3-dimensional manifold, $M(a, b) = \{(a, b) | H_0(a, b) = h_0\}$, obtained by setting $\Theta_a = 0$. In other words, the bounded periodic solutions in Fig. 1 are quasi-periodic orbits on tori, and the hyperbolic fixed points are actually circular periodic solutions.

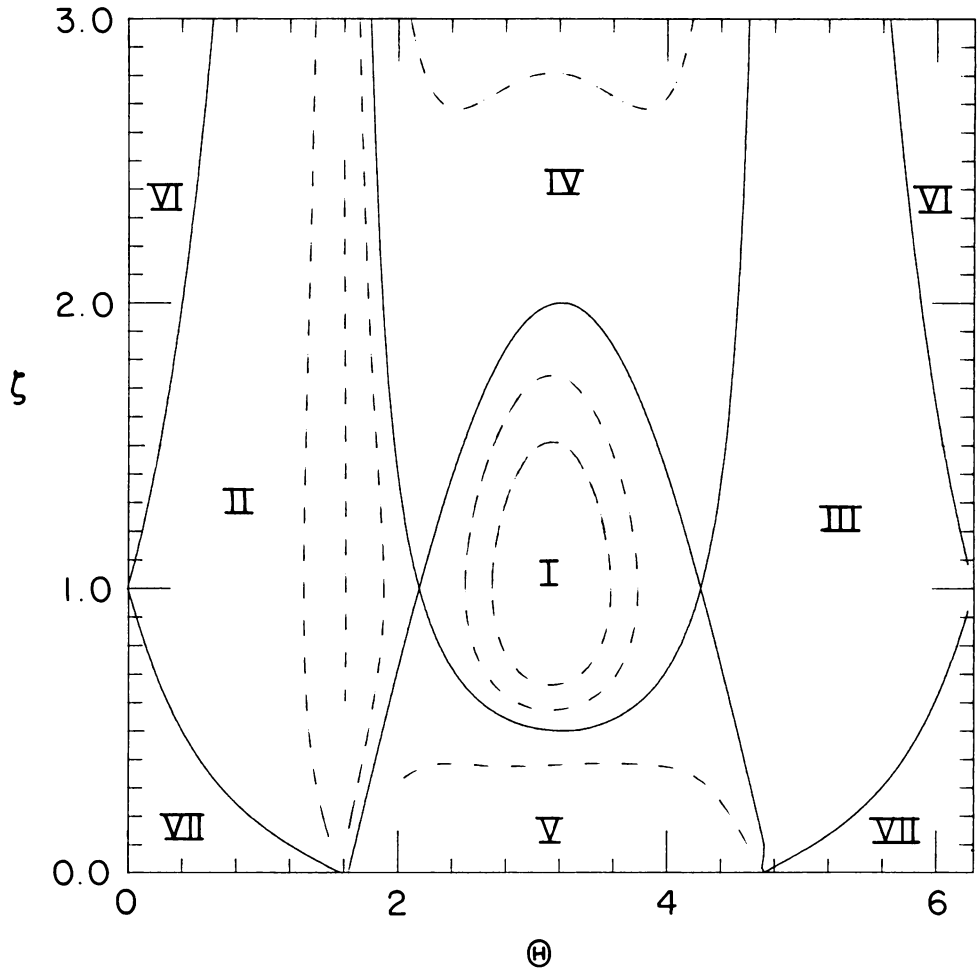

FIG. 1. *Invariant regions.* This illustrates the invariant regions in (ρ, Θ) phase space that characterize the roots of the quartic D (35). The boundaries of these regions are indicated by heavy lines and the verticals $\Theta = \frac{\pi}{2}, \frac{3\pi}{2}$. Representative solutions in each of these regions are shown.

Step II. We will outline the application of the Kolmogorov-Arnold-Moser (KAM) theory [1, 11] to continue the quasi-periodic solutions of (21) to the full equations (18). The Hamiltonian (20) can be put in action-angle form and shown to be real-analytic in the actions away from the singularity, while the perturbation H_1 can be shown to be 2π-periodic in the corresponding angles. Note that $|H_1|$ can be made arbitrarily small by restricting the size of the neighborhood of the singularity (17).

The integrable term H_0 satisfies the KAM nondegeneracy condition in terms of these actions. Finally, the explicit solutions of (21) include a full set of quasi-periodic orbits with two frequencies that satisfy the Diophantine condition [1, 11], i.e., they have strongly-irrational dependence. Thus the KAM theorem implies result (A). The same procedure is used to establish the existence of quasi-periodic solutions in the neighborhood of case 3 and 4 singularities (cf. Secs. 5 and 6).

At the end of this section, we compare the quasi-periodic solutions of the integrable equations (21) to the corresponding numerical solutions of the full equations (1).

The next result:

(B) *Existence of separatrices (heteroclinic orbits) in the phase-space of* (21).

This has important consequences for the dynamics of the von Karman model. The separatrices can be explicitly given in terms of the elliptic integrals that figure in the complete solution of (21). As depicted in Fig. 1, they connect two hyperbolic fixed points and are tangent to the eigenvectors of the Jacobian of (21) at these fixed points.

Upon adding the perturbation H_1, the system (18) cannot be reduced and must be regarded as having two degrees of freedom; hence, Fig. 1 must be interpreted as a Poincaré section. It is well known that the two hyperbolic fixed-points and their stable and unstable manifolds (which formed the separatrices in (21)) persist in the perturbed problem (18). The Melnikov Method [1] can be used to verify their transversal intersection. This involved calculation will not be discussed here (cf. [16]). Generically, these stable and unstable manifolds intersect transversally, leading to horseshoes and chaotic behaviour due to the interlacing of the broken separatrices.

We turn now to the solution of (21). In polar coordinates,

$$a = R_a \exp(i\theta_a), \qquad b = R_b \exp(i\theta_b), \tag{24}$$

(22) takes the form

$$\begin{aligned} \dot{R}_a &= \frac{4h \sin\Theta}{R_b^3}\left(1 + 2\frac{R_b}{R_a}\cos\Theta\right), \\ \dot{R}_b &= \frac{-4h \sin\Theta}{R_a^3}\left(1 + 2\frac{R_a}{R_b}\cos\Theta\right), \\ \dot{\Theta} &= \frac{-4h \cos\Theta}{R_a R_b}\left(\frac{1}{R_a^2} - \frac{1}{R_b^2}\right) \end{aligned} \tag{25}$$

where only the angular difference

$$\Theta = \theta_b - \theta_a \tag{26}$$

appears since (21) is rotationally symmetric about the origin. In essence,

$$h = \frac{R_a^2 R_b^2}{R_a^2 + R_b^2 + 2R_a R_b \cos\Theta} = \text{const} \tag{27}$$

is the Hamiltonian (23). It may be shown directly from (25) that this system has the additional invariant,

$$g = R_a R_b \cos\Theta. \tag{28}$$

From (25), it is clear that

$$\dot{\Theta} = \dot{R}_a = \dot{R}_b = 0 \tag{29}$$

only if

$$R_a = R_b \quad \text{and} \quad \Theta = 0, \pm\frac{2\pi}{3}. \tag{30}$$

Therefore, (25) has three equilibrium points or, equivalently, (21) has three families of circular periodic solutions given by

$$\begin{aligned} &R_a = R_b = R, \qquad \theta_a = \theta_b = \frac{-2\tau}{R^2} + \text{const}, \\ &R_a = R_b = R, \qquad \theta_b = \theta_a \exp\left(\frac{2\pi i}{3}\right) = \frac{4\tau}{R^2} + \text{const}, \\ &R_a = R_b = R, \qquad \theta_b = \theta_a \exp\left(\frac{-2\pi i}{3}\right) = \frac{4\tau}{R^2} + \text{const}. \end{aligned} \tag{31}$$

Note that the frequency of these circular motions becomes arbitrarily large if R is made small.

Since the problem has two invariants, h and g, we can fully integrate (25). In fact if we set

$$x = \cos\theta, \tag{32}$$

we can then obtain

$$\left(\frac{dx}{d\tau}\right)^2 = \frac{16h^2}{g^6}x^4(1-x^2)\left(\left(\frac{g^2}{h} - 2gx^2\right)^2 - 4g^2x^2\right). \tag{33}$$

The solution of (33) can be expressed implicitly in the form

$$t = \frac{g^2}{16h}\int \frac{dX}{X\sqrt{D}} \tag{34}$$

with

$$D = (1-X)(X-p)(X-q)X \tag{35}$$

where $X = x^2$ and

$$\begin{aligned} p &= \frac{1}{2}\left(1 + \frac{g}{h} + \sqrt{1 + \frac{2g}{h}}\right) \\ q &= \frac{1}{2}\left(1 + \frac{g}{h} - \sqrt{1 + \frac{2g}{h}}\right). \end{aligned} \tag{36}$$

All four roots of D are real if and only if

$$1 + \frac{2g}{h} \geq 0. \tag{37}$$

From (27) and (28), it follows that (37) is equivalent to

$$d(\rho, \Theta) = (1 + 4\cos^2\Theta) + 2\cos\Theta\left(\rho + \frac{1}{\rho}\right) \geq 0 \tag{38}$$

where

$$\rho = \frac{R_b}{R_a}.$$

Although (34) can be explicitly evaluated in terms of elliptic integrals, it is more illuminating to sketch trajectories in the (ρ, Θ) phase plane. Since g and h are constants of motion, these are generated by taking $d(\rho, \Theta) = \text{const}$. In Fig. 1, the heavy lines correspond to $d(\rho, \Theta) = 0$ for $\frac{\pi}{2} \leq \Theta \leq \frac{3\pi}{2}$ and $d(\rho, \Theta) = 9$ for $0 \leq \Theta \leq \frac{\pi}{2}$ and $\frac{3\pi}{2} \leq \Theta \leq 2\pi$. The lightly drawn curves give typical trajectories in the (ρ, Θ) phase plane. Thus only in region I do we obtain bounded motions. All other trajectories lead to unbounded solutions of (21). We therefore focus attention on region I where

$$1 \geq X \geq p > q > 0. \tag{39}$$

In this case, the integral in (34) is reduced to (see Byrd and Friedman [3])

$$t = \frac{Ag^2}{16hp}\left[\left(1 - \frac{\mu^2}{k^2}\right)\Pi(\phi, k^2, k) + \frac{\mu^2}{k^2}F(\phi, k)\right] \tag{40}$$

where

$$\phi = \sin^{-1}\left(\frac{(1-q)(X-p)}{(1-P)(X-q)}\right)^{1/2}, \qquad u^2 = \frac{(1-p)}{(1-q)} < 1, \tag{41}$$
$$A = \frac{2}{\sqrt{(1-q)p}}, \qquad k^2 = \frac{(1-p)q}{(1-q)p} < 1.$$

$F(\phi, k)$ and $\Pi(\phi, k^2, k)$ are elliptic integrals of the first and third kinds, respectively. The above motion is periodic and the period is given by

$$T = \frac{Ag^2}{4hp}\left[\left(1 - \frac{\mu^2}{k^2}\right)\frac{E}{1-k^2} + \frac{\mu^2}{k^2}K\right] \tag{42}$$

where K and E are complete elliptic integrals of the first and second kinds. In terms of the phase variables, ρ and Θ, the above periodic solutions of (25) are bounded by

$$\cos^{-1}(-\sqrt{p}) \leq \Theta \leq (2\pi - \cos^{-1}(-\sqrt{p})) \tag{43}$$

and pass through $\Theta = \pi$ twice per period.

We see that in region I, all solutions are periodic. The period T given by (42) is a function of the modulus k, which is defined in (41). As $1 + 2g/h$ tends to zero, the two roots p and q coalesce and the modulus k tends to the value 1. Thus the period T tends to infinity as the Θ amplitude of the periodic solution tends to $\frac{\pi}{3}$. Since equation (25) is defined for the angular difference Θ, the above periodic solutions are essentially quasi-periodic solutions of equation (21). As has been noted before (31), the second period T_2 can be made arbitrarily small by choosing small radii R_a, R_b. Hence the approximate equation (21) has a substantial open set of 2-periodic solutions.

In all other invariant regions, the solutions of (25) become unbounded. We can always choose initial data in an arbitrarily small neighborhood of the singularity (17), which leads to solutions where one of the radii (R_a, R_b) grows linearly in time while the other tends to a small constant. Thus Kochin's equations are nonlinearly unstable at a case 2 singularity. From the solutions in terms of elliptic integrals, it is clear that there are two types of unbounded motions. In regions II and III, the trajectories are monotonic in ρ whereas in regions IV, V, VI, and VII, they are not. By recalling the definition of the variables (18), we interpret the former types of unbounded solutions as the scattering of an approaching vortex trail by a third vortex row where an exchange of partners occurs in the collision. The latter type of unbounded solutions involves a similar scattering process but no exchange of partners occurs in the collision of three vortex rows.

Equation (21), which we have solved completely, is an approximation of Kochin's equation near a case 2 singularity. We now consider how good an approximation it is under various conditions. It is clear that for unbounded solutions, the approximation is valid only on a short time scale. On the other hand, our numerical results indicate that the approximation is a good model for quasi-periodic solutions of Kochin's equation. The plots, Figs. 2 and 3, see pp. 140 and 141, compare numerically the phase trajectories of (21) and Kochin's equations in $(a+b, a-b)$ space. They show that the comparison is very favorable, not only near the singularity as in Fig. 2 but also at some distance from it as in Fig. 3. Since (21) is derived on the assumption that the variables (a, b) are small, it is all the more surprising that it does so well at distances bounded away from the singularity.

The plots of the variable $(a - b)$ in Figs. 2a and 3a show closed curves that resemble circles. The plots of the variable $(a+b)$ indicate more variation in radius. A more effective way to represent these motions is to plot the corresponding Poincaré sections. To be specific, in Fig. 4 (see p. 142), we take Poincaré sections ($a+b$ plane) at $\mathrm{Im}(a-b) = 0$, $\mathrm{Re}(a-b) > 0$ (which correspond to the case in Fig. 2). This verifies that the above solutions of Kochin's equations (and (21)) are essentially 2-periodic and therefore lie on a 2-torus. The above deliberations show that

$$A = \frac{a+b}{2}, \qquad B = \frac{a-b}{2} \tag{44}$$

are the proper coordinates for the quasi-periodic motions of Kochin's equations.

Although a case 2 singularity is unstable, a substantial set of quasi-periodic solutions for (21) has been explicitly obtained. These solutions are very close to the numerical solutions of Kochin's equations and thus account for a class of bounded recurrent motions discussed in paper I. Further, solutions of (21) that leave the neighborhood of the singularity generally satisfy the preconditions (12) or (13) for unbounded motions of Kochin's equations. From the discussion in Sec. 3 and above, this implies that under certain conditions (explicitly given in Fig. 1), a triplet of vortex rows divide into a vortex couple and another row that then separates quickly. This is illustrated in Fig. 6 of paper I.

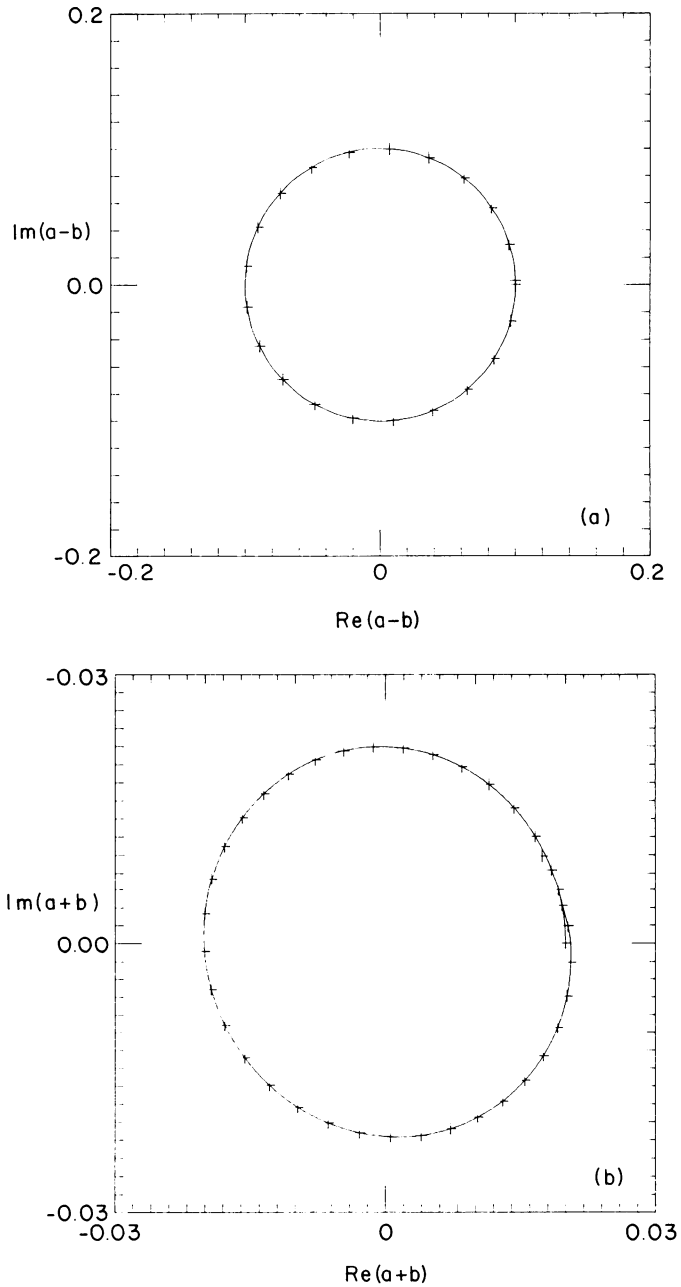

FIG. 2. *Phase plots of* $(a - b, a + b)$. The solutions of (21) and Kochin's equations are compared. For the same initial condition, the full line represents the solution of (21) whereas the crosses represent the solution of Kochin's equations. In this case $|a - b| \approx 0.1$ and $|a + b| \approx 0.02$, which implies that the solution is relatively close to the case 2 singularity (α_0, β_0). For simplicity, in the $(a + b)$-plot only one loop of the phase curve is shown.

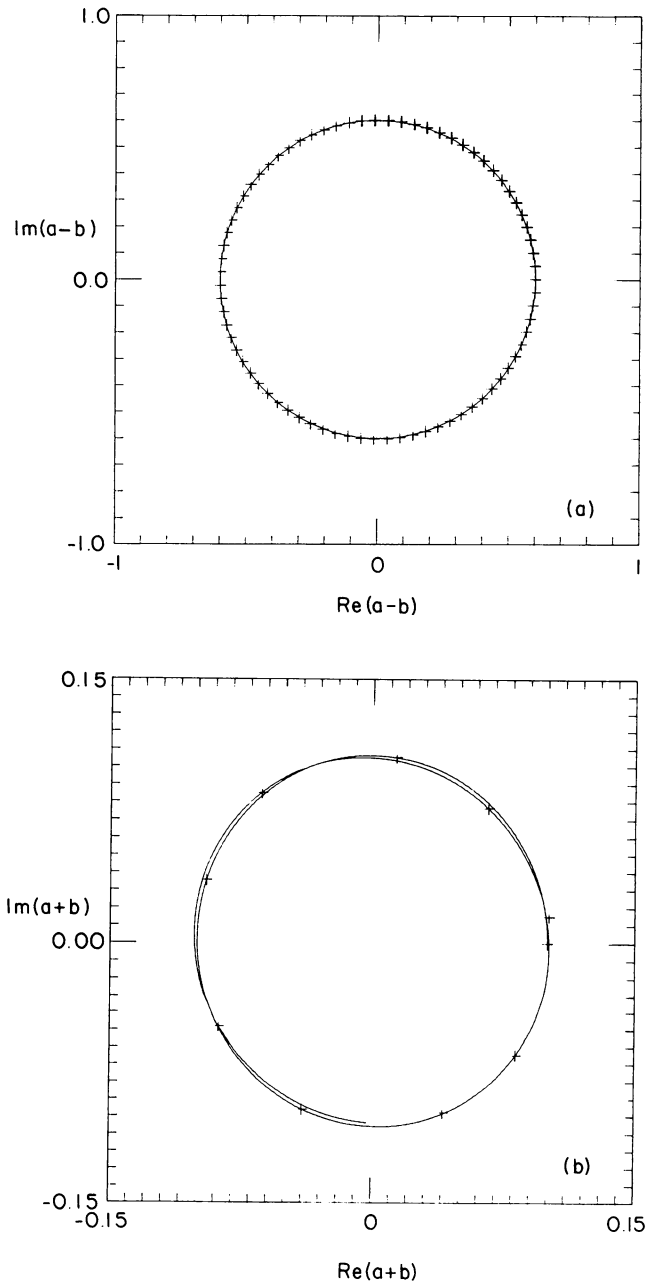

FIG. 3. *Phase plots of* $(a - b, a + b)$. Here $|a - b| \approx 0.6$ and $|a + b| \approx 0.1$, which implies that the solutions of (21) (denoted by full line) and Kochin's equations (denoted by crosses) are bounded away from the singularity.

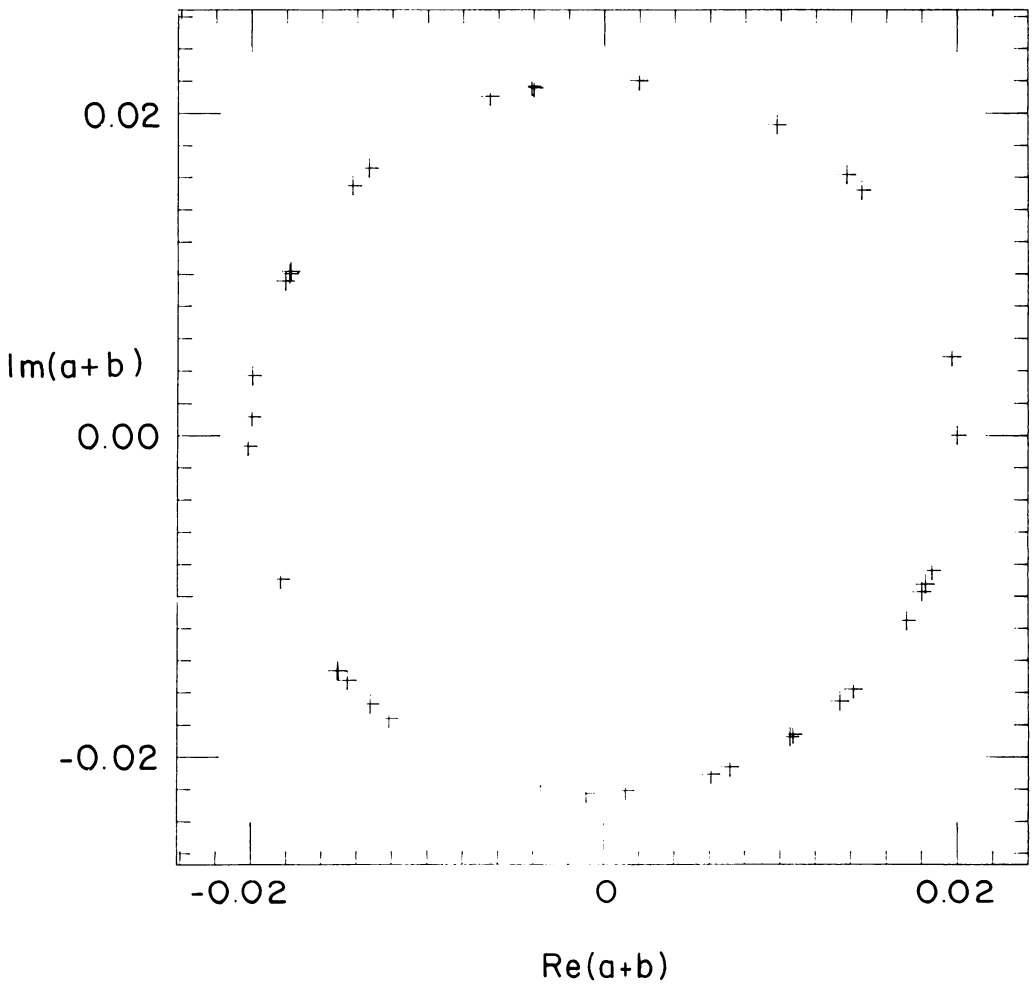

FIG. 4. *Poincaré plot.* A Poincaré section for the solution of Kochin's equations (with same initial data as in Fig. 2) at $\mathrm{Im}(a+b)=0$, $\mathrm{Re}(a+b)>0$ is shown.

5. Vortex merging: Pairing within a triplet. We now consider solutions of Kochin's equations near case 3 singularities where (cf. paper I)

$$\cos\alpha+\cos\beta=0. \tag{45}$$

These singularities correspond to vortex pairing in only one of the two rows in the von Karman trail (cf. Fig. 3c, paper I). The general problem of the motion of such vortex pairs is quite complicated and will not be treated. Instead we focus on the special case of vortex pairs within triplets. Hence the approximate equations (21) form the basis of our discussion in this section. We will show that the new variables (44) are the natural coordinates for quasi-periodic motions and if

$$A\ll B, \quad \text{i.e.,}\ \frac{A}{B}\ll 1, \tag{46}$$

then they are essentially the action-angle variables for (21). Note that (46) follows from the condition (45) for case 3 singularities. If we change to the variables (44) and assume (46), then (21) can be expanded as follows:

$$\dot{\bar{A}} = \frac{2i}{A}\left(\frac{(A+B)^2+(A-B)^2}{A^2-B^2}\right) = \frac{-4i}{A}\left(1+2\frac{A^2}{B^2}+O\left(\frac{A}{B}\right)^3\right), \tag{47}$$

$$\dot{\bar{B}} = \frac{4iB}{A^2-B^2} = \frac{-4i}{B}\left(1+\frac{A^2}{B^2}+O\left(\frac{A}{B}\right)^3\right).$$

The leading terms above give two decoupled ODE's in the new variables

$$\dot{\bar{A}} = \frac{-4i}{A}, \qquad \dot{\bar{B}} = \frac{-4i}{B}. \tag{48}$$

These can be solved directly. First note that

$$\frac{d(A\bar{A})}{d\tau} = \dot{A}\bar{A} + A\dot{\bar{A}} = 0, \tag{49}$$

$$\frac{d(B\bar{B})}{d\tau} = \dot{B}\bar{B} + B\dot{\bar{B}} = 0.$$

Then in polar coordinates for A, B, the equation (48) takes the form

$$\dot{\theta}_a = \frac{4}{R_A^2}, \qquad \dot{R}_A = 0; \tag{50}$$

$$\dot{\theta}_B = \frac{4}{R_B^2}, \qquad \dot{R}_B = 0.$$

Clearly, $J_A = R_A^2$ and $J_B = R_B^2$ are the action variables and θ_A, θ_B are the corresponding angle variables. The solutions of (50) lie on a 2-torus and in general are dense on it except when the two frequencies in (50) are rationally dependent. In terms of the original perturbation variables,

$$a = A + B, \qquad b = A - B, \tag{51}$$

the solutions of (48) are epicycles, i.e.,

$$a = R_B \exp(i\theta_B) + R_A \exp(i\theta_A), \tag{52}$$

$$b = -R_B \exp(i\theta_B) + R_A \exp(i\theta_A)$$

where the radius R_A is much smaller than R_B. This approximates the curves in Fig. 7b of paper I where the ratio of the two frequencies is large. Thus, for the case where the sum A is much smaller than the difference B, the approximate equation (21) (which is completely integrable) takes the simpler form of the weakly coupled equation (47). In view of the discussion in Sec. 4, Kochin's equations can be regarded as perturbations of the decoupled (separable) equations (48). This accounts for the almost circular plots of (A, B) in Figs. 2 and 3.

6. Quasi-periodic solutions near a case 4 singularity: Pairing in both rows of the trail. Next consider solutions of Kochin's equations near the singularities for which

$$\cos\alpha_1 + \cos\beta_1 = 0, \tag{53}$$

$$\sin\alpha_1 = \sin\beta_1 = 0.$$

In particular, we consider the case

$$(\alpha_1, \beta_1) = (\pi, 0). \tag{54}$$

To consider perturbations from the singularity, we write

$$a = \alpha - \pi, \qquad \dot{b} = \beta, \tag{55}$$

in which terms Kochin's equations become

$$\begin{aligned} \dot{\bar{a}} &= \frac{-4i \sin b(-\cos a + i)}{(\cos b - \cos a)(\cos b - i)}, \\ \dot{\bar{b}} &= \frac{4i \sin a(\cos b - i)}{(\cos b - \cos a)(-\cos a + i)}. \end{aligned} \tag{56}$$

Note that the singularity (54) is now given by $(a, b) = (0, 0)$. In addition, all nonzero values for (a, b) such that

$$a = \pm b, \tag{57}$$

are also singular since

$$\cos b - \cos a = 0. \tag{58}$$

On expanding (56) and transforming to

$$A = \frac{a+b}{2}, \qquad B = \frac{a-b}{2}, \tag{59}$$

we obtain

$$\begin{aligned} \dot{\bar{A}} &= \frac{-2i}{A} + \left(2 - \frac{4i}{3}\right) A + O(A^3, B^3), \\ \dot{\bar{B}} &= \frac{2i}{B} - \left(2 - \frac{4i}{3}\right) B + O(A^3, B^3). \end{aligned} \tag{60}$$

If we neglect cubic terms on the right-hand side, the equations decouple and are integrable. To begin with we observe that the leading order

$$\dot{\bar{A}} = \frac{-2i}{A}, \qquad \dot{\bar{B}} = \frac{2i}{B} \tag{61}$$

can be put in action-angle form. To achieve this we take $A = R_a \exp(i\theta_a)$, $B = R_b \exp(i\theta_b)$ so that the above equations become

$$\begin{aligned} \dot{\theta}_a &= \frac{2}{R_a^2} = \frac{-\partial H}{\partial J_a} = \Omega_a, \qquad \dot{J}_a = 0, \\ \dot{\theta}_b &= -\frac{2}{R_b^2} = \frac{-\partial H}{\partial J_b} = \Omega_b, \qquad \dot{J}_b = 0 \end{aligned} \tag{62}$$

where

$$J_a = R_a^2, \qquad J_b = R_b^2 \tag{63}$$

and $H = \ln(J_b/J_a)^2$. Thus $A = J_a \exp(i\Omega_a \tau)$, $B = J_b \exp(i\Omega_b \tau)$ are the solutions and lie on a 2-torus.

We return to (60) with the cubic and higher-order terms dropped. The two resulting equations decouple and are the same under time reversal, and it will be sufficient

to discuss the equation in the variable A. As before, we put the equation in action-angle form

$$\dot{J} = 0 + 4J\cos 2\theta + \frac{8}{3}J\sin 2\theta, \tag{64}$$
$$\dot{\theta} = \frac{2}{J} - 2\sin 2\theta + \frac{4}{3}\cos 2\theta$$

where the subscript a has been dropped. For J small, this is clearly a perturbation of equation (62). In order to solve (64), we divide the two equations to eliminate time:

$$\frac{d\theta}{dJ} = \frac{\frac{1}{J} - F}{J\frac{dF}{d\theta}} \tag{65}$$

where

$$F = \sin 2\theta - \frac{2}{3}\cos 2\theta. \tag{66}$$

After rearranging, we obtain

$$J\frac{dF}{dJ} + F = \frac{d}{dJ}(FJ) = \frac{1}{J}, \tag{67}$$

which has the following solution:

$$F = \sin 2\theta - \frac{2}{3}\cos 2\theta = \frac{\ln CJ}{J} \tag{68}$$

where C is a constant of integration. From (68) it is clear that J is π periodic in θ. Therefore, all solutions like the case before lie on a 2-torus. The frequencies in the solution are large if the corresponding radii are small.

When cubic and higher-order terms in (60) are neglected, the solutions are quasi-periodic. Hence, in the neighborhood of the singularity (54), where the cubic terms are small, the full solutions of (60) should be well approximated by the corresponding quasi-periodic ones. In fact, the results of numerical integration of Kochin's equation indicate that the quasi-periodic solutions (68) are preserved in a neighborhood of the singularity. This is illustrated in Fig. 10 of paper I.

The physical nature of the singularity (54) has been discussed in paper I. For a sketch of the array of vortices corresponding to this singular point, see Fig. 3d of paper I. In these terms, the quasi-periodic solutions above are interpreted as high frequency rotations of pairs of similar vortices. These vortex pairs form staggered arrays with a spacing ratio that is half of that for the Karman trail. An important feature of these solutions is their permanence.

Conclusion. The mathematical analysis of (1) demonstrates that the von Karman model supports a rich variety of large-amplitude spatially periodic solutions. These unbounded and quasi-periodic solutions agree qualitatively with observed large-scale motions of the vortex trail (cf. paper I for more details). Moreover, we have computed explicitly the separatrices (heteroclinic orbits) for the integrable approximate equations (21), which indicate that the von Karman model supports chaotic motions. The results in this paper complete our analysis of question I′: the elegant and simple model proposed by von Karman supports interesting nonlinear solutions, which can be compared with the large-scale motions in vortex trails.

Acknowledgment. The authors take pleasure in acknowledging the unselfish help given to them by Tom Sharp in preparing the figures.

REFERENCES

[1] V. Arnold, *Mathematical Methods of Classical Mechanics*, Springer, New York, 1973
[2] C. Basdevant, Y. Couder, and R. Sadourny, *Vortices and vortex-couples in* 2-D *turbulence*, Lecture Notes in Phys., vol. 157, Springer, 1984, pp. 327–345
[3] P. F. Byrd and M. D. Friedman, *Handbook of Elliptic Integrals for Engineers and Scientists*, 2nd ed., revised, Springer-Verlag, New York-Heidelberg, 1971
[4] N. E. Kochin, I. A. Kiebel, and N. F. Roze, *Theoretical Hydrodynamics*, Wiley Interscience, 1964
[5] H. Lamb, *Hydrodynamics*, Dover, New York, 1945
[6] Chjan C. Lim, *Singular manifolds and quasi-periodic solution Hamiltonians for vortex lattices*, Phys. D **30**, 343–362 (1988)
[7] Chjan C. Lim, *Existence of Kolmogorov-Arnold-Moser tori phase-space of lattice vortex system*, Z. Angew. Math. Phys. **41**, 227–244 (1990)
[8] Chjan C. Lim and L. Sirovich, *Wave propagation on the vortex trail*, Phys. Fluids **29**, 3910–3911 (1986)
[9] Chjan C. Lim and L. Sirovich, *Nonlinear vortex trail* I, Phys. Fluids **31**, 991–998 (1986)
[10] T. Matsui and M. Okude, XV*th International Congress of Theoretical Applied Mechanics*, University of Toronto, Aug. 1980, pp. 1–27.
[11] J. Moser, *Stable and Random Motions*, Princeton Univ. Press, Princeton, NJ, 1973
[12] L. Sirovich, *The Karman vortex trail and flow behind a circular cylinder*, Phys. Fluid **28**, 2723–2726 (1985)
[13] L. Sirovich and Chjan C. Lim, *Comparison of experiment with the dynamics of the von Karman vortex trail*, Studies in Vortex Dominated Flows, Y. Hussaini and M. Salas, eds., Springer-Verlag, New York, 1986, p. 4
[14] S. Taneda, *Downstream development of the wakes behind cylinders*, J. Phys. Soc. Japan **14**, 843–848 (1959)
[15] Th. von Karman, *Über den Mechanismus des Widerstandes, den ein bewegter Körper in einer Flüssigkeit erfährt*, Gottingen Nachr. Math Phys. K **1**, 509–517 (1911)
[16] Chjan C. Lim, *A combinatorial perturbation method and Arnold's whiskered tori in vortex dynamics*, submitted to Physica D.